Nuclear Instruments and Methods in Physics Research B 570 (2026) 165937

Contents lists available at ScienceDirect

Nuclear Inst. and Methods in Physics Research, B

journal homepage: www.elsevier.com/locate/nimb

Evaluation of dosimetric and physical properties of a normoxic polymer gel mimicking bone-tissue

Elif Berna Çalı [a], Ozlem Korkut [b], Alaaddin Gundes [c], Salvatore Gallo [d,*], Mustafa Erdem Sagsoz [e,*]

[a] Ministry of Health Necip Fazil City Hospital, Kahramanmaras 46050, Turkiye
[b] Faculty of Engineering, Chemical Engineering Dept, Atatürk University, Erzurum 25240, Turkiye
[c] Vocational School of Technical Sciences, Sutcu Imam University, Kahramanmaras 46100, Turkiye
[d] Department of Physics and Astronomy "Ettore Majorana", Catania University, via Santa Sofia 64, 95123, Italy
[e] Faculty of Medicine, Biophysics Department, and Askale Vocational School, Atatürk University, Erzurum 25240, Turkiye

ARTICLE INFO

Keywords:
Radiological Tissue-equivalence
Bone
Radiation-therapy
Normoxic polymer hydrogel
Dosimetry

ABSTRACT

Polymer gel dosimeters, recognized for their radiological tissue equivalence, play a crucial role in clinical radiotherapy dosimetry by enabling high-resolution, three-dimensional dose mapping. They allow verification of complex treatment plans and serve as effective tools for quality assurance. Their ability to mimic human tissue and provide spatially resolved dose measurements has been extensively validated in both external beam therapy and brachytherapy. Conventional treatment planning relies on computed tomography (CT) to provide physical and electron density data of the target region. However, CT artifacts caused by metallic implants can compromise dose assessment, highlighting the need for alternative materials that accurately simulate bone tissue. This study presents a bone-equivalent, normoxic polymer gel dosimeter developed to mimic spongy bone tissue. Hydroxyapatite was incorporated into a MAGICA (methacrylic acid and ascorbic acid in gelatin with copper and agarose) formulation to achieve physical properties that closely match those of bone. Key parameters such as mass density (1.190 g cm^{-3}), effective atomic number (10.07) and electron density were consistent with those of trabecular bone, as reported in ICRU Report 44. The linear attenuation coefficients of the gel were experimentally determined at 6 and 15 megavolts (MV) using a linear accelerator (LINAC) system, and the results were in good agreement with theoretical values obtained from XCOM, XMUDAT and Phy-X calculations. These findings confirm the gel's suitability as a bone-equivalent dosimeter with promising applications in radiotherapy research and quality assurance.

1. Introduction

The primary objective of radiation therapy in cancer treatment is to deliver the prescribed dose of radiation precisely to the targeted cancerous tissue while minimizing radiation-induced damage to surrounding healthy tissues and critical organs. With CT imaging, the location, size and surrounding healthy tissues of the targeted volume are mapped. The physical density of the tissues is also important at this stage. Computed Tomography (CT) scans are routinely used during the treatment planning process to provide geometric and physical density information about the anatomical structures within the target volume [1].

Dosimeter devices play a crucial role in this process, measuring the dose of ionizing radiation within their sensitive volume. Gel dosimeters, which are made up of radiation-sensitive chemicals, have attracted attention because they can provide spatially resolved dose measurements.

The spatial resolution of gel dosimeters is directly influenced by the imaging device used for their readout. Since gel dosimeters are tissue-equivalent, they deliver absorbed dose information without requiring correction factors [2]. Furthermore, they offer advantages such as energy independence, dose rate independence, and direction independence, in addition to three-dimensional dose mapping capabilities. Customizable phantoms of desired shapes and sizes can be created by molding these gels.

For over a century, researchers have investigated how radiation

* Corresponding authors.
E-mail addresses: salvatore.gallo@unict.it (S. Gallo), mesagsoz@atauni.edu.tr (M.E. Sagsoz).

https://doi.org/10.1016/j.nimb.2025.165937
Received 30 December 2024; Received in revised form 9 October 2025; Accepted 2 November 2025
Available online 7 November 2025

interacts with human tissues and surrounding materials using tissue-equivalent systems. To be considered tissue-equivalent for photon and electron exposures, a material's radiation absorption and scattering characteristics (for a given thickness or mass) must closely resemble those of biological tissue. Key parameters for evaluating tissue equivalence include the total mass attenuation coefficient (μ/ρ) and the mass energy absorption coefficient (μ_{en}/ρ) for photons, as well as the mass stopping power (S/ρ) and angular scattering power ($\theta^2/\rho l$) for electrons [3]. Combining these radiological properties allows for a detailed understanding of radiation interactions by incorporating the specific weight of the material or, more reliably, the measured specific weight.

The tissue equivalence of materials is often characterized by their effective atomic number (Z_{eff}) and electron density (ρ_e), which depend on chemical composition and energy [4].

Polymer gel dosimeters have emerged as highly valuable tools in clinical radiotherapy dosimetry due to their excellent radiological tissue equivalence and ability to record three-dimensional dose distributions with high spatial resolution. These dosimeters enable accurate mapping of absorbed dose distributions, making them particularly well suited for the verification of advanced and complex treatment plans as well as for routine quality assurance procedures.

Their capacity to replicate the radiological properties of human tissue and deliver spatially resolved dose measurements has been validated in various studies, underscoring their versatility in applications ranging from external beam therapy to brachytherapy.

In medical dosimetry, homogeneous phantoms composed of a single material (*e.g.,* water or PMMA) are commonly utilized for calibration and reference dose measurements. In contrast, anthropomorphic phantoms, which simulate the anatomical and radiological characteristics of the human body, are employed in clinical applications such as mammography, radiotherapy, nuclear medicine, and computed tomography. These phantoms enable the accurate estimation of patient dose under realistic treatment or imaging conditions, thereby enhancing both dosimetric accuracy and patient safety.

In these applications, phantoms imitating the entire human body, a region (thorax, abdomen etc.), an organ or a tissue are produced and modeled [5]. For this purpose, different materials are used for tissues with different densities and properties [6]. In recent years, there have been limited studies that have contributed to soft tissue equivalent polymer gel dosimeters and developed new tissue equivalent polymer gel dosimeters. For example, *Jaszczak et al.* produced a gel dosimeter that imitates bone tissue in terms of density by adding PAGAT2–Pluronic F–127 with hydroxyapatite [7]. Again, *Kumahara et al.* produced a gel dosimeter like bone tissue in terms of density, electron density and effective mass by adding calcium hydrogen phosphate dehydrate to the PAGAT gel dosimeter [8].

In this study, bone-equivalent hydrogel dosimeters were developed by doping MAGICA (Methacrylic and Ascorbic acid in Gelatin Initiated by Copper Agarose addition) hydrogel with micro-sized hydroxyapatite. MAGICA gel is recognized for its minimal deviation in water kerma ratios, making it suitable for water-mimicking applications [9]. Previous studies have produced and characterized bone-equivalent PAGAT (Polyacrylamide Gelatin) gels under atmospheric conditions [7-9].

The physical and dosimetric properties of the developed gel dosimeters were examined to evaluate their tissue equivalence and suitability for radiotherapy applications [10]. To date, limited research has focused on developing polymer gels mimicking bone for photon therapy dosimetry.

Key parameters determined included mass density (ρ), effective atomic number (Z_{eff}), electron density (ρ_e), linear attenuation coefficient (μ), mass attenuation coefficient (μ/ρ), and Hounsfield Units (HU).

This work aims to formulate and characterize a hydroxyapatite-doped MAGICA gel that reproduces the radiological properties of human spongy bone for clinical photon energies.

2. Materials and Methods

2.1. Bone tissue equivalent normoxic polymer gel dosimeter production

The MAGIC gel formulation, as recommended by Fong et al. [11], was employed to produce bone-equivalent normoxic polymer gel dosimeters. The gel mixture was composed of the following components in sequence: 82.3 % w/w ultrapure water (HPLC grade), 8.0 % w/w Type A gelatin (porcine skins, 300 bloom; Fluka, Buchs, Switzerland), 9.0 % w/w methacrylic acid (MAA) (Merck, Darmstadt, Germany), ascorbic acid (2 mmol/L; AFG Bioscience, Northbrook, IL, USA), copper sulfate $CuSO_4{\cdot}5H_2O$ (0.02 mmol/L; ISOLAB, Schweitenkirchen, Germany), and 0.2 % w/w hydroquinone (Acros, Antwerp, Belgium). To improve gel stability, 0.5 % w/w agarose (Apollo Scientific, Cheshire, UK) was incorporated, resulting in a more robust formulation referred to as MAGICA [12]. Micro-sized hydroxyapatite ($Ca_{10}(PO_4)_6$ (OH) $_2$) was added to match the density of spongy bone under standard laboratory conditions (room temperature and atmospheric pressure) (see Table 1).

To prepare 100 g of MAGICA gel dosimeter, based on Fong's MAGIC formula with the additional 0.50 % agarose, the following protocol was followed:

a) Preparation of Gelatin Solution – 8.0 g of porcine gelatin were added to 40 mL of ultrapure water (resistivity 18.2MΩ*cm, obtained by a water purification system Milli-Q® Direct, EMD Millipore) and left to hydrate for 1 h. The hydrated gelatin was dissolved at 50 °C under magnetic stirring until homogeneous. The solution was stirred using a magnetic stirrer until a completely homogeneous mixture was achieved.
b) Preparation of Agarose Solution – In a separate container, 0.5 g of agarose was dissolved in 30 mL of ultrapure water by stirring in a 90 °C water bath. After achieving a homogeneous solution, it was cooled to 50 °C and added to the gelatin mixture.
c) Addition of Hydroquinone – Once the gel container cooled to 50 °C, 0.2 g of hydroquinone dissolved in 5.0 % ultrapure water was added to the mixture. The gel was then allowed to cool further to 37 °C.
d) Incorporation of Ascorbic Acid, Copper Sulfate, and Methacrylic-Acid – The remaining ultrapure water was divided into two parts. One portion was mixed with 0.035 g of ascorbic acid, while the other was combined with 0.0015 g of copper sulfate. These solutions, along with 9 g of Methacrylic-Acid, were added to the gel container at 37 °C. Stirring was continued until a homogeneous mixture was obtained. A mercury thermometer was used to monitor the temperature throughout.
e) Cuvette Filling and Storage – The prepared gel mixture was transferred into 4 mL polypropylene spectrophotometer cuvettes. The gels were stable at room temperature (~23 °C) and were stored in a refrigerator (~4 °C) for 24 h before being transported to the LINAC room for irradiation.

The change of the soft tissue-equivalent MAGICA gel dosimeter into a bone tissue-equivalent gel was achieved by adding micro-sized hydroxyapatite (μHAp; Sigma Aldrich, MA, USA; CAS number: 1306–06-

Table 1
Composition of MAGICA gel dosimeters.

Component	MAGICA	MAGICA+μHap
	Amount (g)	
Gelatin	80	80
Agarose	5	5
Methacrylic acid	90	90
Ascorbic acid	0.352	0.352
$CuSO_4{\cdot}5H_2O$	0.015	0.015
Hydroquinone	2	2
Hydroxyapatite	0	180
Ultra-pure water	823	643

5). Hydroxyapatite, the most abundant inorganic compound in bone tissue, was incorporated to match the physical density and chemical composition of human trabecular (spongy) bone, as defined by ICRU Report 44 [13]. The amount of μHAp added was calculated in direct proportion to replicate these properties accurately. To obtain 100 g of bone tissue equivalent MAGICA, 18 g of HAp was added, and the physical density of the produced sample was found to be 1.190 ± 0.010 g/cm^3 experimentally and was found to be like the trabecular (spongiosa) bone tissue defined in ICRU 44 (1.180 g/cm^3).

To increase the density of the MAGICA gel (initially 1.060 g/cm^3) to match the mass density of human spongy bone tissue (1.180 g/cm^3), a portion of water in the original formula was replaced with micro-sized hydroxyapatite (μHAp). The μHAp used had a particle size of 5 μm and a surface area of ≥ 100 m^2/g. The preparation of the MAGICA gel followed the same procedure as before, with the following modification to incorporate μHAp.

Because hydroxyapatite (HAp) is inherently insoluble in aqueous media, it was dispersed under controlled conditions in a water bath maintained at 37 °C to facilitate even particle distribution. The dispersion procedure was carried out for approximately 5 min, ensuring a homogeneous suspension of μHAp throughout the solution while preserving the constant temperature of 37 °C. To maintain experimental reproducibility and alignment with the initial formulation parameters, the total mass of the resulting gel mixture was standardized to 100 g.

2.2. Mass density measurement

The mass density of the bone-equivalent gel dosimeter was determined using the Archimedes principle [14]. In the study conducted by Aljamal et al. to determine the radiological properties of MACICA gel, the density of the gel was found by Archimedes principle. The gels, which were filled into experimental containers with known volumes at room temperature (~23 °C), were weighed using a laboratory balance (sensitivity of 0.1 mg). The mass density (ρ) was then calculated using the following formula:

$$\rho_{hydrogel} = \frac{m_{hydrogel}}{V_{hydrogel}} \tag{1}$$

where $\rho_{hydrogel}$ represents the mass density of the gel, $m_{hydrogel}$ is the mass of the gel in experiment tube, and $V_{hydrogel}$ is the volume of gel within the experimental container. Shrinkage of the gel was considered when determining the final density. After the gel matrix had formed, the volume $V_{hydrogel}$ was determined by measuring the gel's height. The mass density value $\rho_{hydrogel}$ was experimentally measured and calculated three times for three different gel samples.

2.3. Element composition measurements

To produce bone-equivalent MAGICA gel dosimeters, the following components were used in the proportions outlined in Section 2.1: Type A gelatin (porcine, 300 bloom) ($C_{17}H_{32}N_5O_6$), ascorbic acid ($C_6H_8O_6$), copper sulfate ($CuSO_4{\cdot}5H_2O$), methacrylic acid ($H_2C(CH_3)CO_2H$), ultrapure water, and micro-hydroxyapatite (Ca_{10} $(PO_4)_6$ (OH) $_2$). The weight fractions of the elements carbon (C), hydrogen (H), oxygen (O), nitrogen (N), copper (Cu II), sulfur (S), and phosphorus (P) were determined using the formula described in [15].

$$weightfraction = \frac{mass\ of\ the\ element \in the\ mixture}{mass\ of\ the\ mixture} \tag{2}$$

2.4. Effective atomic number (Z_{eff}) and electron density (ρ_e) measurement

The effective atomic number (Z_{eff}) of the bone-equivalent polymer gel dosimeter was calculated using *Mayneord's formula* [16]:

$$Z_{eff} = \left[\sum_{i=1}^{n} (\alpha_i Z_i^m)\right]^{\left(\frac{1}{m}\right)} \tag{3}$$

For each element, α_i is the electron percentage and Z_i is the electron number [17]. The experimental constant m is 2.94 and is valid for biological materials and water [18]. The electron percentage is calculated using the following formula [18]:

$$\alpha_i = \frac{w_i\left(\frac{Z_i}{A_i}\right)}{\sum w_i\left(\frac{Z_i}{A_i}\right)} \tag{4}$$

The weight fraction of the element is denoted as w_i, and its atomic mass is denoted as A_i.

The electron density corresponds to the probability of finding an electron at a specific location, which is expressed number of electrons N_e per mass of an element:

$$\frac{\rho_e}{\rho} = \frac{N_e}{m} = \frac{ZN_a}{m} = \frac{ZN_A}{A} \tag{5}$$

The unit is e.kg^{-1}. Number of electrons per volume V of an element:

$$\rho_e = \frac{N_e}{V} = Z\frac{N_a}{V} = \rho Z\frac{N_A}{A} \tag{6}$$

The unit *is* $e.m^{-3}$. N_A is Avogadro's number. The number of atoms per gram of an element N_a/m is thus equal to ratio of N_A/A. The element's atomic number is Z, and its atomic mass is A [19].

To calculate the effective electron density of a mixture consisting of different elements, the equation above has been generalized and used in this study [20]:

$$\rho_{eff} = N_A\frac{nZ_{eff}}{\sum_i n_i A_i} = N_A\frac{Z_{eff}}{< A > \left(\frac{electrons}{kg}\right)} \tag{7}$$

where ⟨A⟩ represents the average atomic mass or effective atomic mass of the multi-element material, and n is the number of atoms of element i.

2.5. Measurement of linear (μ) and mass attenuation coefficients (μ/ρ)

To measure the linear attenuation coefficients, radio-chromic film dosimeters were used. First, calibration curves for EBT3 Gafchromic film dosimeters (Ashland® Inc., Bridgewater, USA) were established for 6 MV and 15 MV photon energies, with doses ranging from 100 cGy to 500 cGy (Fig. 1).

The Pixel Value (PV) obtained for each of the energy levels investigated was modeled as a function of the absorbed dose (D) through an exponential regression of the form $PV = A{\cdot}exp(b{\cdot}D)$. In this expression, A serves as a scaling factor reflecting the initial intensity, while b characterizes the rate of exponential decay of PV with increasing dose. The regression analysis demonstrated an excellent fit across all datasets, with correlation coefficients consistently exceeding 0.98, confirming the suitability of the proposed model for describing the PV–dose relationship.

A single scan protocol was used for calibration [21]. The Gafchromic films (3 x 3 cm^2) were then placed under five tissue-equivalent RW3 solid phantoms (Sun Nuclear®, FL, USA), each with a thickness of 1 cm, positioned perpendicular to the direction of the beam at a source-to-surface distance (SSD) of 100 cm, and irradiated with a Varian Clinac® IX linear accelerator (Palo Alto, USA).

Additionally, five different volumes of bone-equivalent MAGICA gel, each with a base size of 4 cm × 4 cm and heights of 1, 2, 3, 4, and 5 cm, were prepared and filled into polypropylene (PP) containers (Fig. 2a-c).

In the same setup, sample containers of equivalent height replaced

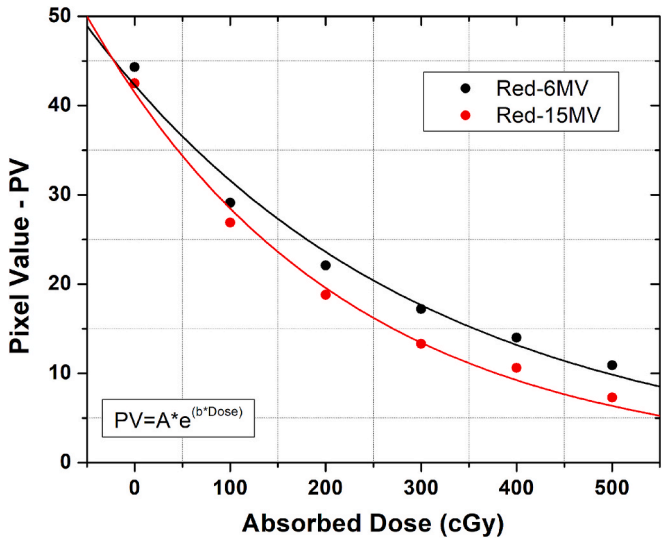

Fig. 1. Film dosimetry calibration curve for 6 MV and 15 MV photon energies. Pixel values (PV) for the different various energy levels considered were fitted as a function of the absorbed dose using an exponential regression of the form $PV = A*\exp(b*Dose)$, where A is a scaling factor, and b represents the decay rate.

the solid phantoms (Fig. 2b and 2c). Gafchromic film dosimeters (3 cm x 3 cm), trimmed to fit the base area of each sample container, were placed beneath the containers. A dose of 200 cGy was delivered to each container. The irradiated film dosimeters were digitized using an Epson Expression 1000XL flatbed scanner (Epson America Inc., Long Beach, CA, USA) with a resolution of 2400 dpi x 4800 dpi and in transmission mode to ensure accurate dose–response acquisition. The scanned images were subsequently analyzed with FilmQA Pro software (version 7, Ashland Inc., Bridgewater, NJ, USA) to calculate the net optical density by subtracting the background signal and converting pixel intensity values into dose–response data [22]. During both the calibration curve development and sample irradiation, a dose rate of 300 cGy/min. was maintained. The linear attenuation coefficient of the bone-equivalent MAGICA hydrogel was then determined using the Beer-Lambert law.

$$I = I_0 e^{-\mu x} \tag{8}$$

I, is the intensity of the emerging radiation, I_0, is the intensity of the incoming photons, μ times the thickness, x, of the material through which the incoming radiation passes. For a mixture consisting of different elements, the total mass attenuation coefficient is the sum of the attenuation coefficients of the elements that compose the material [23].

$$\frac{\mu}{\rho} = \sum_i w_i \left(\frac{\mu}{\rho}\right)_i \tag{9}$$

Here, w_i represents the weight fraction of the i-th element in the mixture, and $(\mu/\rho)_i$ is the mass attenuation coefficient of the i-th element. The experimental results obtained were compared with the theoretical results obtained using XCOM [24], XMUDAT [25] and Phy-X software [26].

The XCOM program is a comprehensive database and computational tool designed to calculate the mass attenuation coefficients of atoms, compounds, and mixtures with atomic numbers below 100 over an energy range from 1 keV to 100 GeV. Within this energy range, XCOM can determine both partial mass attenuation coefficients such as those due to Compton scattering, the photoelectric effect, and pair production and total mass attenuation coefficients. For the analysis of bone tissue-equivalent gel dosimeters, the "mixture" tab on the program's main interface is selected, and the weight fraction of each constituent element is entered. By specifying the desired photon energies, the program then provides the corresponding partial and total mass attenuation coefficients, allowing for detailed characterization of the material's interaction with ionizing radiation.

The XMUDAT software is a computational tool used to calculate mass attenuation coefficients, electron densities, and effective atomic numbers for atoms, compounds, and mixtures over a photon energy range of 1 keV to 50 MeV. For the analysis of bone tissue-equivalent gel dosimeters, the "mixture" tab on the program's main interface is selected, and the weight fraction of each constituent element is entered. By specifying the desired photon energies, the software then computes both partial and total mass attenuation coefficients, providing detailed information on the interaction of radiation with the material. This approach enables precise characterization of the dosimeter's radiological properties, which is essential for accurate dosimetric assessments.

Phy-X/ZeXTRa software can calculate the total mass attenuation coefficient and energy absorption parameters because of the interaction of atoms with atomic numbers up to 92 with photons in the energy range of 1 keV to 20 MeV. In addition, the total stopping power can be calculated because of the interaction of charged particles such as electrons, protons, alpha particles and carbon ions with atoms with atomic numbers up to 92 in the energy range of 1 keV to 1 GeV.

On the starting page of the software, the weight fraction for each

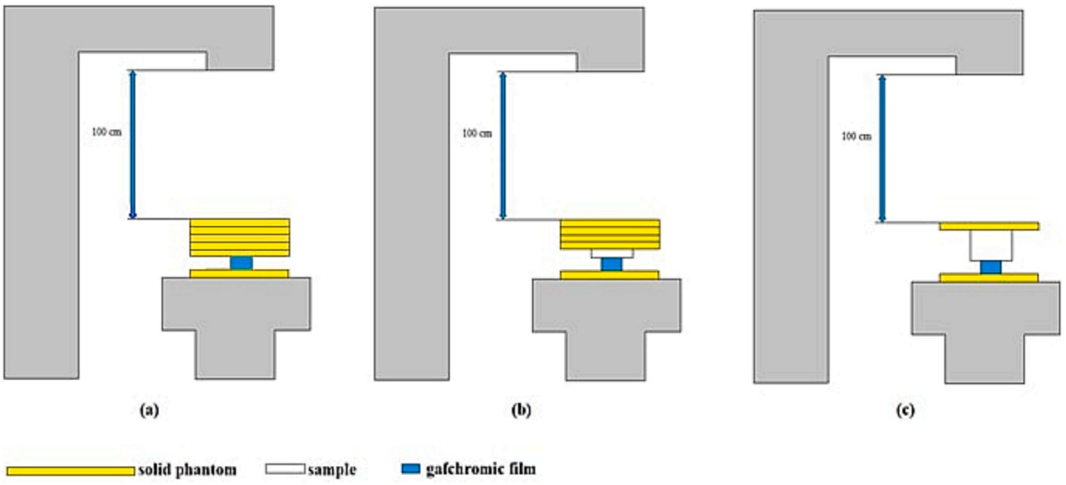

Fig. 2. Schematic illustration of the experimental setup inside the LINAC room (not to scale). Yellow boxes represent water-equivalent thicknesses; the dosimetry gel is shown in white, and the radiochromic film in blue. (a) Setup for the calibration of the Gafchromic film; (b) Dose measurement through a 1 cm-high sample; (c) Dose measurement through a 4 cm-high sample. In both (b) and (c), the dose is recorded by the Gafchromic film after transmission through the sample.

element that makes up the bone tissue equivalent gel dosimeter is entered. The sum of the weight fractions equals 1. Photon was chosen as the radiation type of interest. Atomic number (Z)-Photon Interaction (ZPI) was chosen to calculate the total photon interaction based on the X-ray mass attenuation coefficient (XMAC).

2.6. CT scan of MAGICA Gel, Bone-Equivalent MAGICA Gel, and Water-Filled sample Vials

Computed tomography (CT) imaging was performed using an Aquilion® LB multi-slice CT scanner (Toshiba, Nasu, Japan). The study utilized 4.0 cm^3 spectrophotometer cuvettes containing MAGICA gel, bone-equivalent MAGICA gel, and water, alongside an empty container assumed to represent air. Scans were acquired using a head and neck imaging protocol with a 700 mm field of view (FOV), a 512 × 512 reconstruction matrix, 120 kVp tube voltage, and 300 mAs tube current. A slice thickness of 1 mm was applied for all acquisitions, ensuring high spatial resolution and accurate characterization of the phantom materials.

2.7. Irradiation procedure and MRI scanning

The bone-equivalent hydrogels were poured into spectrophotometer cuvettes and stored at + 4 °C for 24 h to reach thermal equilibrium before being transferred to the LINAC room. During irradiation and subsequent scanning or measurements, the gels were maintained at approximately 23 °C.

For each irradiation, the LINAC was calibrated in accordance with the IAEA TRS-398 code of practice (IAEA 2000) [27] using an Ionization Chamber (CI). For the calibration, the CI was positioned in a water phantom at a depth of 10 cm, using as reference conditions a source–surface distance of 100 cm and a field size 10 cm × 10 cm, for all the x-ray beam energies.

The gel sample containers were positioned at the isocenter, with a Source Surface Distance (SSD) of 100 cm and a field size of 10 cm x 10 cm, while the gantry was set to 0°. Each sample was irradiated individually. One container was kept aside without irradiation to serve as a background reference.

To generate the dose–response curve of the bone tissue-equivalent hydrogel, computed tomography (CT) images were imported into the treatment planning system (TPS), and the monitor unit (MU) value required to deliver the prescribed dose to the center of the gel phantom was calculated. Treatment planning was performed using the Eclipse™ v13.6 treatment planning system (Varian Medical Systems, Palo Alto, CA, USA). The gel samples were irradiated using a Varian Clinac® IX linear accelerator (Palo Alto, USA), delivering doses of up to 40 Gy at a rate of 300 cGy/min with a photon energy of 6 MV. Afterwards, the samples were wrapped in aluminum foil to block light and stored in a refrigerator at + 4 °C for 24 h prior to MRI scanning.

After irradiation and refrigeration, the gel samples were brought to the MRI room, where they were allowed to equilibrate thermally at ~ 23 °C for approximately 10 h. MR images of the irradiated gel samples were acquired using a 1.5 T Signa Explorer® MRI device (GE, Milwaukee, USA) with an RF head coil. The imaging protocol included a Repetition Time (T_R) of 4040 ms, Echo Times (T_E) of 113 ms and 123 ms. The parameters were chosen both following the literature and to maximize image-contrast [28]. To obtain the dose–response curve, three independently prepared samples were irradiated under identical conditions at the same dose levels on separate occasions. Corresponding MR images were acquired for each irradiation, and the variability between measurements remained consistently below 5 %.

3. Results and Discussion

3.1. Basic characteristics of dosimeter

The mass density of the bone-equivalent gel dosimeter has been experimentally measured to be 1.190 ± 10 g/cm^3. This parameter is essential for accurately mimicking the density of bone tissue.

The elemental compositions of different gel formulations, including MAGICA and MAGICA+μHAp, were determined. These gel dosimeters were designed to closely mimic the composition of human bone tissue. Comparison of these compositions with actual bone materials, such as skeletal spongiosa, confirms their tissue-equivalent properties.

The effective atomic number (Z_{eff}) and electron density (ρ_e) of the gel dosimeters were calculated, providing critical information for their use in radiation therapy simulations. The values obtained indicate that these gel dosimeters closely resemble the radiation interactions realized in human bone tissue (Table 2, Table 3 **and** Table 4).

Experimental measurements of mass attenuation and linear attenuation coefficients for the gel dosimeter were compared with results calculated using XCOM, XMUDAT and Phy-X programs. The close agreement between experimental and calculated values underscores the accuracy and reliability of these dosimeters in simulating radiation interactions (Table 5).

The experimental linear attenuation coefficients were determined as 0.030 ± 0.002 cm^{-1} at 6 MV and 0.020 ± 0.001 cm^{-1} at 15 MV, while the mean theoretical values (XCOM, XMUDAT, Phy-X) were 0.033 cm^{-1} at 6 MV and 0.024 cm^{-1} at 15 MV. Although the absolute deviations were only 0.003–0.004 cm^{-1}, they correspond to relative differences of approximately 9 % (6 MV) and 17 % (15 MV). These discrepancies can be explained by the expected uncertainty of radiochromic film dosimetry, typically reported as ± 5–10 % depending on calibration, energy dependence, and scanner reproducibility [29–32], as well as by the photon spectrum of clinical linac beams, which differs from the monoenergetic assumptions used in theoretical datasets [27,33]. The linear attenuation coefficient (μ) was experimentally measured using film dosimetry for 6 MV and 15 MV photon energies. Based on the obtained results, a thickness versus relative dose graph was plotted (Fig. 3), and the linear attenuation coefficient (μ) for 6 MV and 15 MV photon energies was determined using the Lambert-Beer principle.

The logarithm of the intensity ratios versus gel thickness was fitted using linear regression. For the energies considered, the fitting model showed very good correlation with the data, with r^2 values greater than 0.998, indicating consistency within the experimental uncertainty.

The bone tissue-equivalent gel dosimeters, irradiated up to 40 Gy with a 6 MV photon energy produced by linear accelerators used in clinics, were obtained by processing the images from a magnetic resonance imaging (MRI) device using ImageJ software [34] and measured values with a rectangular Region of Interest (ROI).

A linear regression analysis was performed to evaluate the relationship between absorbed dose and R_2. Linear regression analysis was conducted using least-squares fitting (OriginPro v2024). The results demonstrated a significant dose–response relationship ($p < 0.05$), confirming that the observed increase was statistically significant at the 95% confidence level. The p-value was obtained from the *t*-test statistic of the slope coefficient relative to its standard error. The dose–response curve of the bone-equivalent gel dosimeter indicates a potential to provide dose information, suggesting that with further validation it could become a useful tool in radiation therapy studies. (Fig. 4) [35].

Furthermore, the electron density and effective mass calculated for MAGICA and bone tissue-equivalent gel using the PhyX/ZeXTRA program were found to be very close to the values defined for soft tissue and trabecular bone in ICRU 44 [13] (Fig. 5).

The MAGICA+μHAp bone-equivalent gel dosimeter demonstrates good promise as a tool for simulating radiation interactions in human bone tissue, especially spongy bone. This formulation combines the benefits of normoxic polymer gel technology with hydroxyapatite

Table 2
The elemental composition of MAGIC gel, MAGICA gel, MAGICA+μHAp, water and human skeleton spongiosa.

Material	w_C	w_H	w_O	w_N	w_{Ca}	w_P	w_{Cu}	w_S
MAGIC[a]	0.075	0.1062	0.8120	0.014	0.000	0.000	5.08×10^{-6}	2.58×10^{-6}
MAGICA	0.095	0.104	0.787	0.014	0.000	0.000	5.08×10^{-6}	2.58×10^{-6}
MAGICA+μHap	0.095	0.086	0.698	0.014	0.072	0.033	5.08×10^{-6}	2.58×10^{-6}
SKELETON SPONGOISA[b]	0.404	0.085	0.361	0.028	0.074	0.034	0.000	0.000
WATER	0.000	0.111	0.888	0.000	0.000	0.000	0.000	0.000

[a] (Fong et al., 2001) [11] [b](ICRU 44) [13].

Table 3
Mass density, electron density, number of electrons per gram and effective atomic number for MAGIC gel, MAGICA gel, MAGICA+μHAp, water, human skeleton spongiosa.

Material	ρ ($g\ cm^{-3}$)	ρ_e ($x\ 10^{29}\ e\ m^{-3}$)	ρ_e/ρ ($x10^{26}\ e\ kg^{-1}$)	Z_{eff}
MAGIC[a]	1.060	3.51	3.310	7.07
MAGICA	1.037	3.44	3.323	7.30
MAGICA+μHap	1.190 ± 2	3.90	3.28	10.07
SKELETON SPONGIOSA[b]	1.180	3.84	3.26	9.85
WATER	1.000	3.34	3.34	7.22

[a] (Fong et al., 2001) [11] [b].

doping, to provide radiological and dosimetric equivalence to human spongiosa bone tissue.

The measured Hounsfield Unit (HU) value of 360 ± 4 exhibits strong agreement with the reference values reported in the literature for spongy (trabecular) bone, thereby validating the reliability of the proposed formulation as a bone-equivalent material [34].

The detailed investigation of the MAGIC+μHAp hydrogel revealed properties consistent with human bone, including its elemental composition, mass density, electron density, number of electrons per unit volume, effective atomic number, and linear attenuation coefficient. These parameters collectively demonstrate that the gel effectively reproduces the radiological response of spongiosa bone tissue. Consequently, the MAGIC+μHAp hydrogel can be regarded as a robust radiological and dosimetric surrogate, broadening its applicability in radiation therapy dosimetry, treatment verification, and phantom-based experimental studies.

In contrast to previous studies employing PAGAT gels doped with magnesium chloride or hydroxyapatite precursors for bone mimicry, the present work introduces a non-toxic, normoxic MAGICA gel matrix doped with hydroxyapatite (μHAp). Notably, the linear attenuation coefficient of the MAGIC+μHAp gel was determined at clinically relevant therapeutic x-ray energies, addressing a significant limitation of earlier research that utilized non-clinical energy ranges. This approach eliminates the need for energy-dependent corrections when evaluating tissue equivalency under therapeutic x-ray conditions. Such characterization is essential for developing materials suitable for use in radiotherapy applications [8,36–45].

Additionally, we have experienced that hydroxyapatite is an ideal material for creating bone tissue equivalent gel dosimeters, as it shows low solubility and high stability at 37 °C and slightly higher

Table 4
Mass Absorption Coefficient (MAC), Linear absorption coefficient (LAC), number of electron per gram (ρ_e/ρ) and effective atomic number (Z_{eff}) for MAGICA+ μHAp gel and human skeleton spongoisa change with photon energy calculated by Phy-X program [26].

MAGICA +μHAp **Z_{eff}**	SPONGOI SA BONE **Z_{eff}**	MAGICA +μHap ***ρ_e/ρ*** *electrons/g*	SPONGOI SA BONE ***ρ_e/ρ*** *electrons/g*	MAGICA +μHap **LAC** *1/cm*	SPONGOI SA BONE **LAC** *1/cm*	MAGICA +μHAp **MAC** *cm^2/g*	SPONGOI SA BONE **MAC** *cm^2/g*	MATERIAL AL **Energy** *MeV*
10.48	10.53	8.89E + 23	9.26E + 23	2.194	2.081	1.844	1.764	2.00E-02
6,15	5,94	5,21E + 23	5.22E + 23	0.473	0.458	0.397	0.388	4.00E-02
4.73	4.54	4.01E + 23	4.00E + 23	0.287	0.281	0.241	0.38	6.00E-02
4.27	4.10	3.62E + 23	3.61E + 23	0.234	0.230	0.196	0.195	8.00E-02
3.89	3.75	3.30E + 23	3.29E + 23	0.161	0.159	0.135	0.135	2.00E-01
3.86	3.71	3.27E + 23	3.27E + 23	0.123	0.122	0.104	0.104	4.00E-01
3.85	3.71	3.27E + 23	3.26E + 23	0.104	0.103	0.087	0.087	6.00E-01
3.85	3.71	3.26E + 23	3.26E + 23	0.091	0.090	0.077	0.077	8.00E-01
3.85	3.70	3.26E + 23	3.26E + 23	0.082	0.081	0.069	0.069	1.00E + 00
3.87	3.72	3.28E + 23	3.27E + 23	0.057	0.057	0.048	0.048	2.00E + 00
3.97	3.81	3.37E + 23	3.35E + 23	0.040	0.039	0.034	0.033	4.00E + 00
4.10	3.93	3.48E + 23	3.45E + 23	0.033	0.032	0.028	0.027	6.00E + 00
4.24	4.05	3.59E + 23	3.56E + 23	0.029	0.028	0.024	0.024	8.00E + 00
4.37	4.16	3.71E + 23	3.66E + 23	0.027	0.026	0.022	0.022	1.00E + 01
4.67	4.43	3.96E + 23	3.89E + 23	0.024	0.023	0.020	0.019	1.50E + 01

Table 5
Experimental Measurements of Mass Attenuation and Linear Attenuation Coefficients of Bone-Equivalent MAGICA Gel Dosimeter Compared with Results Calculated Using XCOM, XMUDAT and Phy-X Programs.

	Linear Attenuation Coefficients μ (cm^{-1})				*Mass Attenuation Coefficients* (μ/ρ) (cm^2/g)			
	MAGICA + μHAP		SPONGOISA		MAGICA + μHAP		SPONGOISA	
	6 MV	15 MV	6 MV	15 MV	6 MV	15 MV	6 MV	15 MV
Experimental	0.030	0.020	–	–	0.025	0.017	–	–
XCOM	0.033	0.024	0.032	0.023	0.028	0.018	0.027	0.020
XMUDAT	0.032	0.024	0.032	0.023	0.027	0.020	0.027	0.020
Phy-X	0.033	0.024	0.032	0.023	0.028	0.020	0.027	0.019

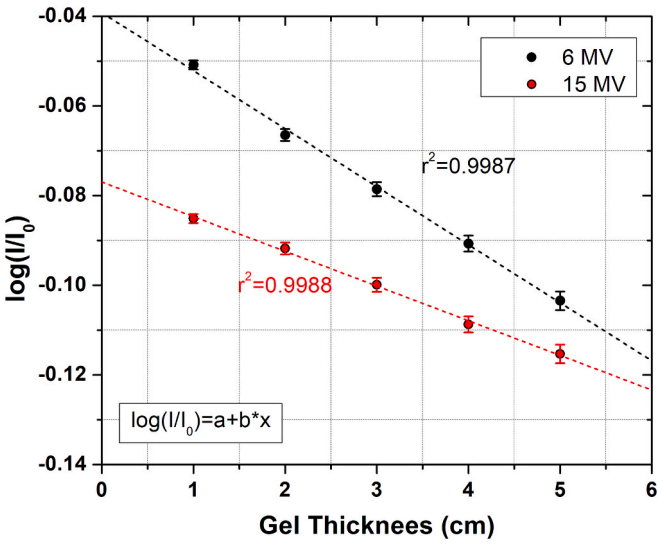

Fig. 3. Relative dose variation versus gel thickness for 6 MV and 15 MV photon energies. A linear regression was applied to the logarithm of the ratio I/I_0 as a function of gel thickness (x).

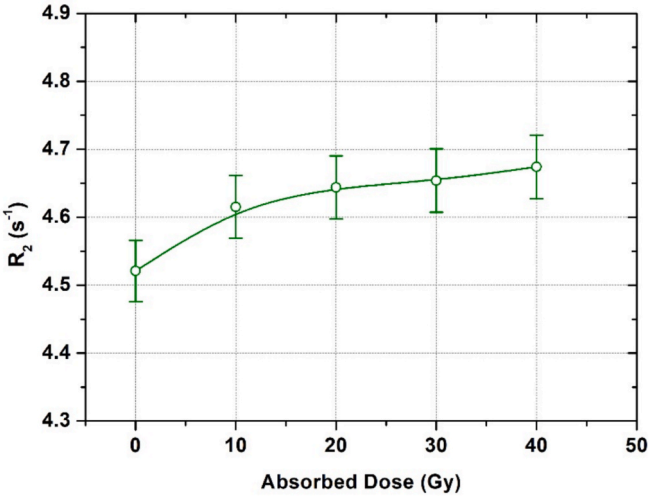

Fig. 4. Bone-Equivalent Gel Dosimeter Dose-Response Curve.

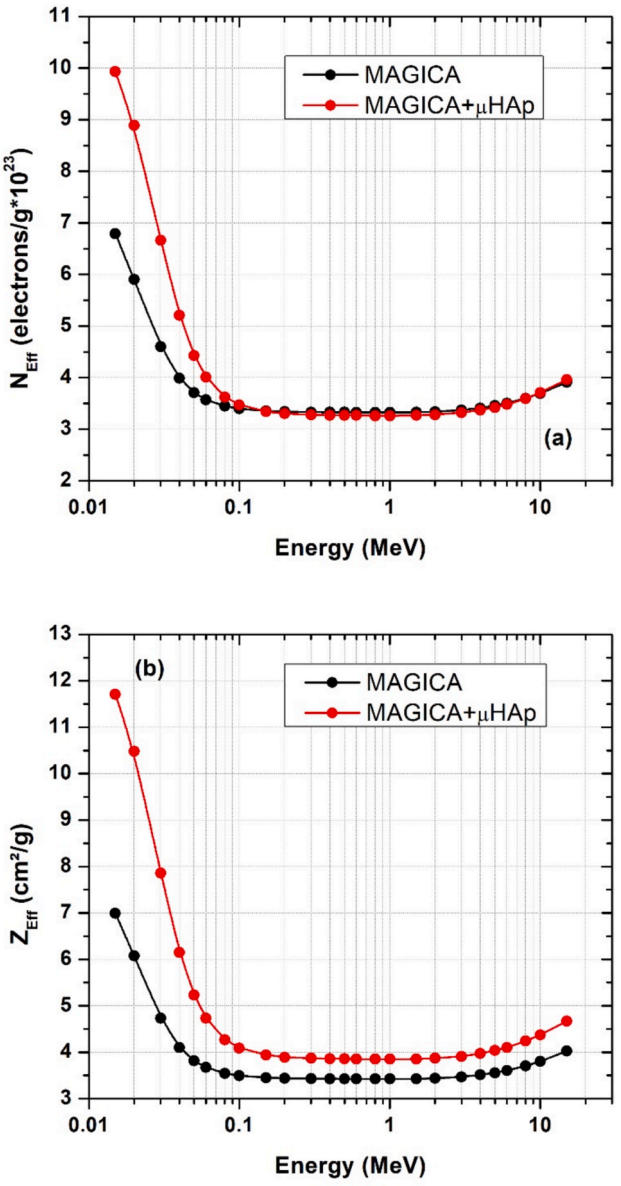

Fig. 5. MAGICA and bone-equivalent gel dosimeter electron density (a) and Z_{eff} (b) curves.

temperatures. These properties ensure long-term reliability in biological environments [46–48].

Finally, the linear attenuation coefficient was determined at clinically relevant treatment energies, which differ from those employed in previous studies.

4. Conclusions

The MAGIC+μHAp gel dosimeter mimic the response of bone tissue to radiation, integrating the adaptable properties of MAGIC gel with the bone-mimicking characteristics of micro-structured hydroxyapatite (μHAp).

This hydrogel exhibits radiological and dosimetric parameters that are consistent with those of trabecular bone, including Z_{eff}, ρ_e and HU values.

This advanced composition results in a superior dosimetric system with enhanced tissue equivalence. It is particularly valuable in radiotherapy applications, supporting more precise treatment planning and promising improved clinical outcomes.

Future investigations will focus on assessing the material's dose linearity, temporal stability and overall imaging compatibility, with the aim of ensuring its clinical viability.

CRediT authorship contribution statement

Elif Berna Çalı: Writing – review & editing, Writing – original draft, Visualization, Software, Resources, Project administration, Methodology, Investigation, Funding acquisition, Formal analysis, Data curation, Conceptualization. **Ozlem Korkut:** Writing – review & editing, Writing – original draft, Supervision, Software, Resources, Data curation, Conceptualization. **Alaaddin Gundes:** Writing – review & editing, Writing – original draft, Visualization, Validation, Formal analysis, Data curation, Conceptualization. **Salvatore Gallo:** Writing – review & editing, Visualization, Validation, Supervision, Software, Resources, Conceptualization. **Mustafa Erdem Sagsoz:** Writing – review & editing, Writing – original draft, Visualization, Validation, Supervision, Investigation, Formal analysis, Data curation, Conceptualization.

Declaration of competing interest

The authors declare that they have no known competing financial interests or personal relationships that could have appeared to influence the work reported in this paper.

Acknowledgments

We extend our thanks to Ahmet Kürşat Özkan for his contribution to the film dosimetry analysis. This study is supported by Atatürk University BAP TDK-2021-9328. The English of this manuscript was improved using an AI-assisted language editing tool. The authors are fully responsible for the scientific content.

Data availability

Data will be made available on request.

References

[1] S. Puvanasunthararajah, D. Fontanarosa, M.L. Wille, S.M. Camps, The application of metal artifact reduction methods on computed tomography scans for radiotherapy applications: a literature review, J. Appl. Clin. Med. Phys. 22 (6) (2021) 198–223, https://doi.org/10.1002/acm2.13274.

[2] R. Dhakal, M. Yosofvand, H. Moussa, Development and application of MAGIC-f gel in cancer research and medical imaging, Appl. Sci. 11 (17) (2021) 7783, https://doi.org/10.3390/app11177783.

[3] J. Venning, B. Brindha, C. Baldock, Preliminary study of a normoxic PAG gel dosimeter with tetrakis (hydroxymethyl) phosphonium chloride as an antioxidant, J. Phys. Conf. Ser. 3 (2004) 155–158, https://doi.org/10.1088/1742-6596/3/1/019.

[4] M. Kurudirek, Water and tissue equivalence properties of biological materials for photons, electrons, protons, and alpha particles in the energy region 10 keV–1 GeV: a comparative study, Int. J. Radiat Biol. (2016), https://doi.org/10.1080/09553002.2016.120622.

[5] M. Wegner, E. Gargioni, D. Krause, Classification of phantoms for medical imaging, Procedia CIRP 119 (2023) 1140–1145, https://doi.org/10.1016/j.procir.2023.03.154.

[6] N. Okkalidis, et al., A filament 3D printing approach for CT-compatible bone tissues replication, Physica Medica: European Journal of Medical Physics 102 (2024) 96–102.

[7] M. Jaszczak-Kuligowska, et al., Towards optimisation of the chemical composition of a bone-imitating dosimeter as a potential component of multiphase dosimeters, J. Phys. Conf. Ser. 2799 (2024) 012006, https://doi.org/10.1088/1742-6596/2799/1/012006.

[8] N. Kumahara, A. Takemura, S. Ishihara, et al., Sensitivity of a bone-equivalent polymer gel dosimeter for measuring the dose to bone during radiation therapy, Radiol. Phys. Technol. 16 (2023) 227–234, https://doi.org/10.1007/s12194-023-00710-9.

[9] M. Kozicki, M. Jaszczak-Kuligowska, P. Maras, Measurement of ionising radiation dose absorbed by bones using a bone-imitating polymer gel dosimeter, Measurement 240 (2025) 115633, https://doi.org/10.1016/j.measurement.2024.115633.

[10] E. Pantelis, A.K. Karlis, M. Kozicki, P. Papagiannis, L. Sakelliou, J.M. Rosiak, Polymer gel water equivalence and relative energy response with emphasis on low photon energy dosimetry in brachytherapy, Phys. Med. Biol. 49 (2004) 3495–3514, https://doi.org/10.1088/0031-9155/49/15/006.

[11] M. Fong, C. Keil, D. Does, C. Gore, Polymer gels for magnetic resonance imaging of radiation dose distributions at normal room atmosphere, Phys. Med. Biol. 46 (2001) 3105–3113, https://doi.org/10.1088/0031-9155/46/11/309.

[12] Zahmatkesh, M. H., Kousari, R., Akhlaghpour, S., & Bagheri, S. A. (2004). MRI gel dosimetry with methacrylic acid, ascorbic acid, hydroquinone and copper in agarose (MAGICA) gel. Preliminary Proceedings of DOSGEL, 2004.

[13] D.R. White, J. Booz, R.V. Griffith, J.J. Spokas, I.J. Wilson, ICRU report 44, Journal of the International Commission on Radiation Units and (1989). Measurements.

[14] M. Aljamal, et al., Polymer gels in radiation therapy: Characterization and applications, J. Phys. Conf. Ser. 423 (2013) 012016, https://doi.org/10.1088/1742-6596/423/1/012016.

[15] J.V. Trapp, G. Michael, Y. De Deene, C. Baldock, Attenuation of diagnostic energy photons by polymer gel dosimeters, Phys. Med. Biol. 47 (2002) 4247–4258, https://doi.org/10.1088/0031-9155/47/23/306.

[16] W.V. Mayneord, The significance of the roentgen, Acta International Union against Cancer 2 (1937) 271–282.

[17] M.M. Goodsitt, E.G. Christodoulou, S.C. Larson, Accuracies of the synthesized monochromatic CT numbers and effective atomic numbers obtained with a rapid kVp switching dual energy CT scanner, Med. Phys. 38 (2011) 2222–2232, https://doi.org/10.1118/1.3571571.

[18] S. Manohara, S. Hanagodimath, K. Thind, L. Gerward, On the effective atomic number and electron density: a comprehensive set of formulas for all types of materials and energies above 1 keV, Nucl. Instrum. Methods Phys. Res., Sect. B 266 (18) (2008) 3906–3912, https://doi.org/10.1016/j.nimb.2008.06.034.

[19] M. Kurudirek, Effective atomic numbers, water and tissue equivalence properties of human tissues, tissue equivalents and dosimetric materials for total electron interaction in the energy region 10 keV-1 GeV, Appl. Radiat. Isot. 94 (2014) 1–7, https://doi.org/10.1016/j.apradiso.2014.07.002.

[20] J.E. Physics for Radiation Protection, 3rd ed.; Wiley-VCH: Weinheim, 2006. https://doi.org/10.1002/9783527618798.

[21] D. Lewis, A. Micke, X. Yu, M.F. Chan, An efficient protocol for radiochromic film dosimetry combining calibration and measurement in a single scan, Med. Phys. 39 (2012) 6339–6350, https://doi.org/10.1118/1.4754797.

[22] M. Mathot, S. Sobczak, M.T. Hoornaert, Gafchromic film dosimetry: four years experience using FilmQA pro software and Epson flatbed scanners, Phys. Med. 30 (8) (2014) 871–877.

[23] Hubbell, H. And S. M. Seltzer, Tables of X-ray Mass Attenuation Coefficients and Mass Energy-Absorption Coefficients 1 keV to 20 MeV for Elements Z=1 to 92 and 48 Additional Substances of Dosimetric Interests National Institute of Standards and Technology, U.S. Department of Commerce, Gaithersburg, MD, 1995d. 17J.

[24] Berger, M.J.; Hubbell, J.H.; Seltzer, S.M.; Chang, J.; Coursey, J.S.; Sukumar, R.; Zucker, D.S.; Olsen, K. XCOM: Photon Cross Section Database (version 1.5). Natl. Inst. Stand. Technol. 2010. Available online: http://physics.nist.gov/xcom (accessed on 11 September 2024).

[25] Nowotny, R. XMuDat Photon attenuation data on PC, Version 1.0.1, Nuclear Data Service, IAEA: Vienna, Austria, 1998.

[26] E. Şakar, Ö.F. Özpolat, B. Alım, M.I. Sayyed, M. Kurudirek, Phy-X/PSD: development of a user-friendly online software for calculation of parameters relevant to radiation shielding and dosimetry, Radiat. Phys. Chem. 166 (2020) 108496.

[27] Andreo, P.; Burns, D.; Hohlfeld, K.; Huq, M.; Kanai, T.; Laitano, F.; Smyth, V.; Vynckier, S. (2000). Absorbed Dose Determination in External Beam Radiotherapy: An International Code of Practice for Dosimetry Based on Standards of Absorbed Dose to Water (IAEA Technical Reports Series) vol. 398, International Atomic Energy Agency.

[28] J.C. Gore, Y.S. Kang, R.J. Schulz, Measurement of radiation dose distributions by nuclear magnetic resonance (NMR) imaging, Phys. Med. Biol. 29 (1984) 1189–1197.

[29] Devic S, Seuntjens J, Sham E, Podgorsak EB, Schmidtlein CR, Kirov AS, Soares CG. Precise radiochromic film dosimetry using a flat-bed document scanner. Med Phys. 2005 Jul;32(7Part1):2245-2253. PMID: 28493574.

[30] M.J. Butson, T. Cheung, P.K. Yu, Measurement of energy dependence for XRCT radiochromic film, Med. Phys. 33 (8) (2006 Aug) 2923–2925, https://doi.org/10.1118/1.2219330. PMID: 16964870.

[31] A. Niroomand-Rad, C.R. Blackwell, B.M. Coursey, K.P. Gall, J.M. Galvin, W. L. McLaughlin, A.S. Meigooni, R. Nath, J.E. Rodgers, C.G. Soares, Radiochromic film dosimetry: recommendations of AAPM Radiation Therapy Committee Task Group 55. American Association of Physicists in Medicine, Med. Phys. 25 (11) (1998 Nov) 2093–2115. PMID: 9829234.

[32] D. Lewis, A. Micke, X. Yu, M.F. Chan, An efficient protocol for radiochromic film dosimetry combining calibration and measurement in a single scan, Med. Phys. 39 (10) (2012 Oct) 6339–6350, https://doi.org/10.1118/1.4754797. PMID: 23039670; PMCID: PMC9381144.

[33] Marroquin EY, Herrera González JA, Camacho López MA, Barajas JE, García-Garduño OA. Evaluation of the uncertainty in an EBT3 film dosimetry system utilizing net optical density. J Appl Clin Med Phys. 2016 Sep 8;17(5):466-481. PMID: 27685125; PMCID: PMC5874103.

[34] N. Birur, P. Praveen, G. Sanjana, G. Keerthi, et al., Comparison of gray values of cone-beam computed tomography with Hounsfield units of multislice computed tomography: an in vitro study, Indian J. Dent. Res. 28 (2017) 66–70.

[35] C.T. Rueden, J. Schindelin, M.C. Hiner, et al., ImageJ2: ImageJ for the next generation of scientific image data, BMC Bioinf. 18 (2017) 529, https://doi.org/10.1186/s12859-017-1934-z.

[36] S. Gallo, S. Locarno, E. Brambilla, C. Lenardi, E. Pignoli, I. Veronese, Dosimetric characterization of double network Fricke hydrogel based on PVA-GTA and phenylalanine peptide derivative, J. Phys. D Appl. Phys. 57 (7) (2023) 075303, https://doi.org/10.1088/1361-6463/ad0987.

[37] M. Sedighi, E. Edalatkhah, P. Taherparvar, Characterization of ferrous-xylenol orange-polyvinyl alcohol gel for gamma dosimetry using spectroscopy, Radiochim. Acta 112 (11) (2024) 923–928.

[38] M. Kozicki, M. Jaszczak, P. Maras, Features of PABIGnx 3D Polymer Gel as an Ionising Radiation Dosimeter, Materials 15 (7) (2022) 2550, https://doi.org/10.3390/ma15072550.

[39] S. Gallo, E. Artuso, M.G. Brambilla, G. Gambarini, C. Lenardi, A.F. Monti, I. Veronese, Characterization of radiochromic poly (vinyl-alcohol)–glutaraldehyde Fricke gels for dosimetry in external x-ray radiation therapy, J. Phys. D Appl. Phys. 52 (22) (2019) 225601, https://doi.org/10.1088/1361-6463/ab08d0.

[40] S. Ceberg, T. Olding, C. Baldock, Gel dosimetry has a viable future for dosimetry in the radiation oncology clinic, Phys. Eng. Sci. Med. 47 (1) (2024) 1–5.

[41] M.L. Jensen, C.L. Nielsen, M.B. Jensen, L.P. Muren, R.M. Turtos, B. Julsgaard, P. Balling, A Tissue-Equivalent, Reusable Dosimeter for 3D Verification of Radiotherapy, Adv. Funct. Mater. 2412587 (2024).

[42] C.P. Karger, A. Elter, S. Dorsch, P. Mann, E. Pappas, M. Oldham, Validation of complex radiotherapy techniques using polymer gel dosimetry, Phys. Med. Biol. 69 (6) (2024) 06TR01.

[43] N. Sheykholeslami, W. Parwaie, V. Vaezzadeh, M. Babaie, M. Farzin, G. Geraily, A. H. Karimi, Dual application of polyvinyl Alcohol Glutaraldehyde Methylthymol

Blue Fricke hydrogel in clinical practice: Surface dosimeter and bolus, Appl. Radiat. Isot. 197 (2023) 11082.
[44] S. Gallo, S. Pasquale, C. Lenardi, I. Veronese, A.M. Gueli, Effect of ionizing radiation on the colorimetric properties of PVA-GTA Xylenol Orange Fricke gel dosimeters, Dyes Pigm. 187 (2021) 109141, https://doi.org/10.1016/j.dyepig.2021.109141.
[45] M.E. Sagsoz, O. Korkut, S. Gallo, Advancements in Tissue-Equivalent Gel Dosimeters. Gels 11 (2) (2025) 81, https://doi.org/10.3390/gels11020081.
[46] T. Kokubo, H. Takadama, How Useful Is SBF in Predicting in Vivo Bone Bioactivity?biomaterials 27 (15) (2006) 2907–2915, https://doi.org/10.1016/j.biomaterials.2006.01.017.
[47] H. Pan, B.W. Darvell, Determination of the solubility of hydroxyapatite by solid titration, Arch. Oral Biol. 52 (11) (2007) 977–982.https://doi.org/10.1016/j.archoralbio.2007.04.005.
[48] Poorhemati, A., & Komarova, S. V. (2023). A mathematical model of hydroxyapatite precipitation in the interstitial fluid of bone tissue. Frontiers in Applied Mathematics and Statistics, 9, 1294540. https://doi.org/10.3389/fams.2023.1294540.